

# Magnetic properties of Quantum Corrals from first-principles calculations

B. Lazarovits<sup>††</sup>, B. Újfalussy<sup>‡</sup>, L. Szunyogh<sup>†§</sup>, B. L. Györffy<sup>†\*</sup> and P. Weinberger<sup>†</sup>

**Abstract.** We present calculations for electronic and magnetic properties of surface states confined by a circular quantum corral built of magnetic adatoms (Fe) on a Cu(111) surface. We show the oscillations of charge and magnetization densities within the corral and the possibility of the appearance of spin-polarized states. In order to classify the peaks in the calculated density of states with orbital quantum numbers we analyzed the problem in terms of a simple quantum mechanical circular well model. This model is also used to estimate the behaviour of the magnetization and energy with respect to the radius of the circular corral. The calculations are performed fully relativistically using the embedding technique within the Korringa-Kohn-Rostoker method.

<sup>††</sup>Center for Computational Materials Science, Technical University Vienna, A-1060, Gumpendorferstr. 1.a., Vienna, Austria

<sup>‡</sup>Metals and Ceramics Division, Oak Ridge National Laboratory, Oak Ridge, Tennessee 37831, USA

<sup>§</sup> Department of Theoretical Physics and Center for Applied Mathematics and Computational Physics, Budapest University of Technology and Economics, Budafoki út 8, H-1111, Budapest, Hungary

<sup>\*</sup> H. H. Wills Physics Laboratory, University of Bristol, Bristol BS8 1TL, United Kingdom

## 1. Introduction

Over the past two decades, electrons in two-dimensional (2D) surface states on closed packed surfaces of noble metals have been at the center of much experimental and theoretical attention [1, 2]. For a pristine surface the energies of such states lay in the 'gap' around the L point of the bulk Brillouin Zone and the wavefunctions are confined to the surface. The corresponding dispersion relations have been determined by angle resolved photoemission spectroscopy and they have been found to be 2D free-electron like parabolas [1, 3]. Moreover, they are partially filled and hence the electrons, which fill them, form a 2D metal. The most interesting feature of this remarkable state of matter is its response to perturbations such as caused by placing transition metal atoms on the surface. As might be expected, such response displays long range, 'Friedel like', charge oscillations governed by the 2D Fermi 'Surface'. Indeed, one of the iconic experiments in nano-technology has been the fabrication of a circular arrangement of 48 Fe atoms on a Cu (111) surface and the direct observation, by Scanning Tunneling Microscopy (STM), of such oscillations within the circle [4, 5, 6]. In this paper we wish to discuss the, as yet unexplored, magnetic properties of such quantum corrals.

<sup>†</sup> To whom correspondence should be addressed. E-mail: bl@cms.tuwien.ac.at

Until recently STM studies of atoms on well defined Cu, Ag and Au (111) surfaces imaged only the charge distribution of the surface electrons [4, 5, 6]. But now, remarkable developments in spin-polarized STM (SPSTM) [7] make the observing of spatial variations in the magnetic density a distinct possibility and, therefore, an attractive new area of research. Evidently, this opens up the possibility of building magnetic nanostructures for both scientific and technological purposes. For instance, while the observation of a single Fe or Co atom on a Cu surface may be beyond the spatial resolution of the first generation of SPSTMs, the magnetic state of a single quantum corral of 50-100 atoms can be readily identified [8]. The motivation behind the theoretical work reported here is the need to identify the principle conceptual issues which govern the physics, in general, and the magnetism, in particular, of such structures.

Individual impurities and clusters of impurities embedded in the above surface-2D-host-metals have been studied for Friedel oscillations around them [9, 10], for RKKY interactions between them [11, 12, 13] and for a rich variety of Kondo-like phenomena they are host to [6, 14, 15, 16]. Clearly, all these effects can occur inside a corral with the interesting aspect that now the electronic structure of the host can be controlled by the geometry of the corral. It is perhaps useful to note that these circumstances are rather analogous to that of quantum wells in semiconductor physics [17].

In the semiclassical limit the states of the quantum corrals can be associated with classical orbits of particles bouncing off confining walls. Depending on the shape of the corral the classical motions may be integrable or chaotic. Thus, quantum corrals can serve as examples of quantum chaos at work [18, 19].

Clearly, to think about using different impurities, different substrates and/or different confining geometries one needs simple but reliable models as guides. In the unfamiliar physical circumstances at hand, an efficient way to such models is to perform large scale first-principles calculations including all conceivably relevant effects and in interpreting the results in terms of simple models. This is the approach we take in the present paper. Our first-principles calculations are a spin-polarized and relativistic generalization of the pioneering work of Hörmandinger and Pendry [2] and Crampin and collaborators [20, 21]. We interpret our results in terms of a flat bottom 'circular potential well', non-relativistic, model. To illustrate the power of this approach, once it has been established that the model faithfully reproduces the main features of the results from first-principles calculations, properties which would be too difficult to calculate from first principles are estimated.

## 2. Method of calculations

Within multiple scattering theory of the electronic structure the information about each atom (scattering center) is coded in the scattering path operator (SPO) matrix,  $\tau(E) = \{\underline{\tau}^{nm}(E)\} = \{\tau_{QQ'}^{nm}(E)\}$ , with  $Q$  and  $Q'$  being angular momentum indices referring to atomic sites whose position vectors are labeled by  $n$  and  $m$ , respectively, and  $E$  being the energy. For scatterers described by non-overlapping (muffin-tin) potential wells, the SPO matrix,

$$\tau(E) = [\mathbf{t}^{-1}(E) - \mathbf{G}(E)]^{-1} \quad , \quad (1)$$

describes the full hierarchy of scattering events between any two particular sites,  $n$  and  $m$ . In Equation (1),  $\mathbf{t}(E) = \{\underline{t}^n(E) \delta_{nm}\} = \{t_{QQ'}^n(E) \delta_{nm}\}$  and  $\mathbf{G}(E) = \{\underline{G}^{nm}(E)\} =$

$\{G_{QQ}^{nm}(E)\}$  denote the single-site  $t$ -matrices on the energy shell and the real-space structure constants, respectively [23].

We begin our investigations by two fully self-consistent calculations: one for a semi-infinite Cu with a (111) surface and another one for a single Fe adatom on this semi-infinite host. In the first case, above the Cu layers there are two layers of sites occupied by atomic cells without nuclear charge which we call empty sites, but we note that they do contain electronic charge and their electrostatic potential is calculated fully self-consistently. In the second type of self-consistent calculation, one empty site above the topmost Cu layer is occupied by an Fe atom. We then construct 'crystal potentials' for further single pass, one-electron calculations according to the following recipe: within the corresponding atomic spheres, all Fe sites are described by the potential as obtained from the single impurity calculation and all other sites are described by the appropriate potentials from the pristine surface calculation. The configurations of interest are those in which some empty sites in the layer above the topmost Cu layer are replaced by Fe atoms, forming thus the wall of a corral as shown in Figure 1. Clearly, by this construction, at the level of the 'crystal potential', we are neglecting the influence of neighbouring Fe atoms on each other. Fortunately, this 'frozen potential' approximation was shown to be reasonable in the case of Fe adatoms on Ag(100) [24].

For a given 'crystal potential' constructed according to the above recipe we solve the multiple scattering problem by means of the embedding method [24]. In short, we embed a cluster of sites labeled by  $\mathcal{C}$ , consisting of the corral Fe atoms and selected empty sites inside and outside the corral, in the unperturbed semi-infinite Cu host. A particular cluster  $\mathcal{C}$  can then be treated as perturbation of the host. In practice, we first calculate the SPO matrix of the 2D translational invariant layered host,  $\tau_h(\mathbf{k}_{\parallel}, E) = \{\tau_h^{pq}(\mathbf{k}_{\parallel}, E)\}$ , within the framework of the SKKR method [25], where  $p$  and  $q$  denote layers and the  $\mathbf{k}_{\parallel}$  are vectors in the surface Brillouin zone (SBZ). The real-space SPO matrix is then given by

$$\tau_h^{mn}(E) = \frac{1}{\Omega_{SBZ}} \int_{SBZ} e^{-i(\mathbf{T}_i - \mathbf{T}_j)\mathbf{k}_{\parallel}} \tau_h^{pq}(\mathbf{k}_{\parallel}, E) d^2k_{\parallel} \quad , \quad (2)$$

where the atomic position vectors are decomposed as  $\mathbf{R}_m = \mathbf{T}_i + \mathbf{c}_p$  and  $\mathbf{R}_n = \mathbf{T}_j + \mathbf{c}_q$  with  $\mathbf{T}_i$  and  $\mathbf{T}_j$  being 2D lattice vectors,  $\mathbf{c}_p$  and  $\mathbf{c}_q$  the so-called layer-generating vectors, and  $\Omega_{SBZ}$  is the unit area of the surface Brillouin zone.

By replacing the  $t$ -matrices of the unperturbed host,  $t_h(E)$ , with those of the cluster-atoms,  $t_{\mathcal{C}}(E)$ , leads to the following Dyson like equation,

$$\tau_{\mathcal{C}}(E) = \tau_h(E) [\mathbf{I} - (t_h^{-1}(E) - t_{\mathcal{C}}^{-1}(E))\tau_h(E)]^{-1} \quad , \quad (3)$$

where  $\tau_{\mathcal{C}}(E)$  is the SPO matrix corresponding to all sites in cluster  $\mathcal{C}$ , from which in turn local quantities, such as the densities of states (DOS), magnetic densities of states (MDOS), spin and orbital moments, as well as the total energy can be calculated. Note, that Equation (3) takes into account all scattering events both inside and outside the cluster.

### 2.1. Geometries of interest

The 48 Fe atoms forming the corral were positioned on the surface along a circle with a diameter of 28  $a$ , where  $a$  is the 2D lattice constant of the fcc(111) Cu surface. The investigated geometry is shown in the inset of Figure 1. This is similar to a popular

experimental one [4]. The corral sites refer to the positions of an ideal fcc parent lattice with the experimental Cu lattice constant, therefore, there is some deviation from the exact circular shape. The positions of the adatoms were chosen such that the spacing between them is approximately constant. Within the interior of the corral the physical properties (DOS, MDOS) of 55 empty spheres along a diameter were calculated. Note that the rotational symmetry of the considered structure is not continuous. Nevertheless, to reduce the computational effort, we followed Crampin *et al.* [20] and assumed that the properties on an arbitrary position within the corral depend only on the distance from the center of the circle.

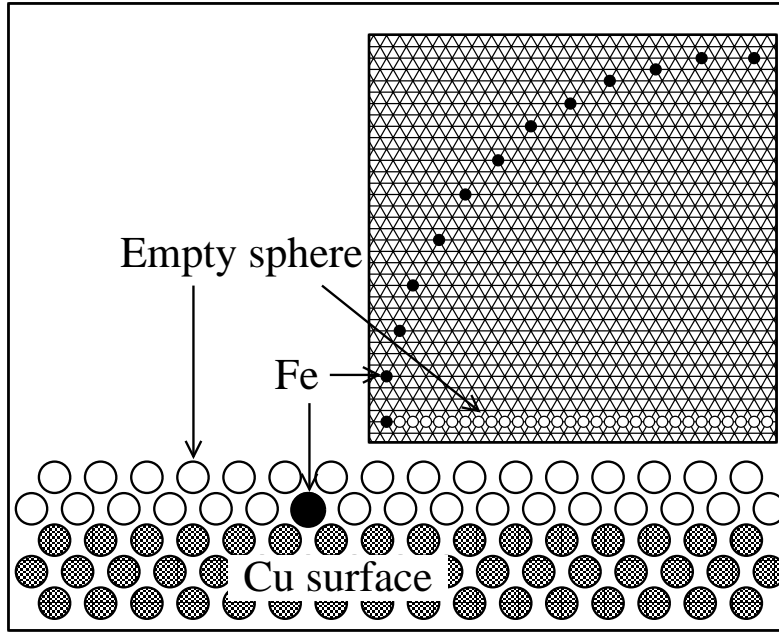


**Figure 1.** Cross section of the surface showing the position of sites in the 'vacuum layers' (open circles), the Cu surface layers (gray circles) and an Fe impurity in the first 'vacuum layer' (black circle). Inset: the positions of the Fe atoms (black dots) and the empty spheres (open circles) along a diameter for a quadrant of the investigated corral.

## 2.2. Computational details

Self-consistent, fully relativistic calculations for the pristine Cu(111) surface as well as for the Fe adatom on Cu(111) have been performed in the framework of the local spin-density approximation (LSDA) as parameterized by Vosko *et al.* [27]. The potentials were treated within the atomic sphere approximation (ASA). For the calculation of the  $t$ -matrices and for the multipole expansion of the charge densities, necessary to evaluate the Madelung potentials, a cut-off of  $\ell_{max} = 2$  was used. The energy integrations were performed by sampling 16 points on a semicircular contour in the complex energy plane according to an asymmetric Gaussian quadrature. Both for the self-consistent calculation of the Cu(111) surface and for the evaluation of Equation (2) we used 70  $k_{\parallel}$ -points in the irreducible wedge of the SBZ (ISBZ). The DOS and MDOS were calculated at an energy mesh parallel to the real axis with an imaginary

part of 0.5 mRyd. In here, in order to cover the surface-state properties properly, a sampling of about 3300  $k_{\parallel}$ -points within the ISBZ was necessary.

### 3. Results of first-principles calculations

#### 3.1. Clean Cu(111) surface

In order to determine the dispersion relation and the effective mass of the surface electrons the *Bloch-spectral function* (BSF) [23] was calculated between  $\bar{\Gamma}$  and  $\bar{K}$  in the fcc(111) SBZ close to the Fermi energy by using the SKKR method, in which the properties of the semi-infinite substrate are calculated by the surface Green function method [25]. The proper treatment of the host is necessary to account for the interaction between the bulk and surface states in an ab-initio way. The maxima of the BSF can be identified as the surface state band. In agreement with the experiments, the calculated dispersion relation is free-electron like and can be estimated with a parabola as indicated in Figure 2. The bottom of the calculated surface states band,  $E_B$ , is 0.3 eV below the Fermi energy which is a bit smaller than the experimental value (0.39 eV) [1, 3]. By using a quadratic approximation for the dispersion relation,

$$E(\mathbf{k}_{\parallel}) = E_B + \frac{\hbar^2 k_{\parallel}^2}{2m^*} + \dots \quad , \quad (4)$$

we obtained an effective mass with  $m^* = 0.366 m_e$  which is in good agreement with the experiment ( $m^*/m_e \approx 0.41$ ) [3].

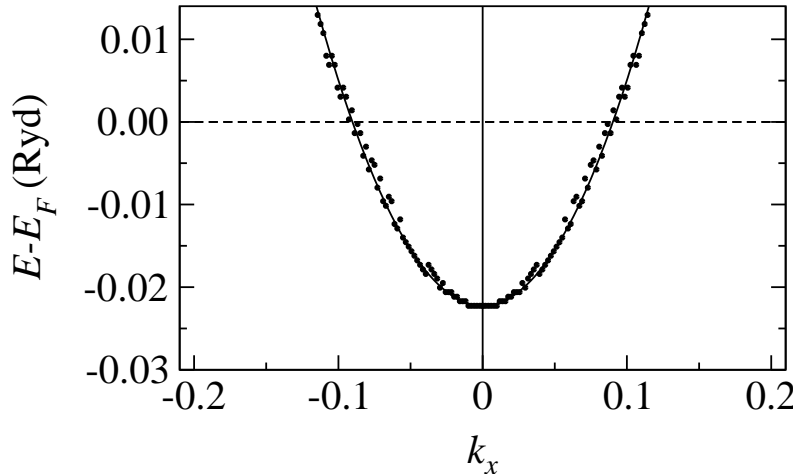


**Figure 2.** Dots: Bloch spectral function maxima near to the  $\bar{\Gamma}$  point of the SBZ. Line: parabola fitted to the calculated maxima. It should be noted that only the first third of the SBZ is displayed ( $\bar{K} \approx 0.65/a.u.$ ). The estimated effective mass is  $m^* = 0.366 m_e$ .

#### 3.2. Fe impurity on a Cu(111) surface

In these calculations the magnetic moment of the Fe impurity on the surface turned out to be  $3.27 \mu_B$  and, due to the magneto-crystalline anisotropy (MCA) induced

by spin-orbit coupling [28], its preferred orientation was perpendicular to the surface. The MCA energy, defined as the difference of the LSDA total energy between an in-plane and a normal-to-plane orientation of the magnetization, yielded 4.3 meV. Both of these results are consistent with those already reported in the literature [26]. We note that the orientation of the magnetic moments in the quantum corral built up from Fe atoms is, in principle, also affected by the so-called shape anisotropy, arising from the magnetostatic dipole-dipole energy [28]. This, purely classical, interaction would direct the orientations of the magnetic moments into the plane. According to our estimates, the magnetostatic dipole-dipole energy is, however, at least by one order less in magnitude than the above MCA energy. Therefore, in our further calculations the Fe adatoms were taken to be spin-polarized in the  $z$  direction, i.e., normal to the surface. Moreover, the exchange (RKKY) interaction between two Fe atoms can be both ferro- and antiferromagnetic depending on the distance between them. This implies that by varying the geometry of the corral various ground-state magnetic configurations can occur. Because of experimental interest, in this work we have studied the case of a ferromagnetic corral.

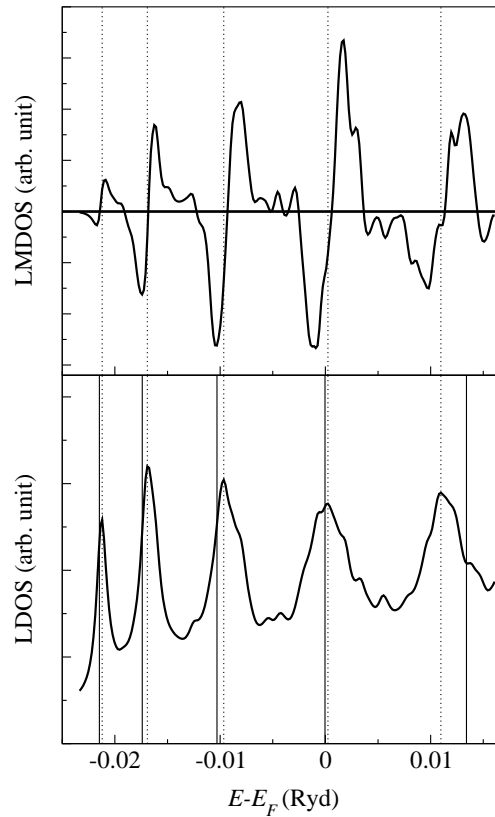


**Figure 3.** Calculated local density of states (LDOS) and local magnetic density of states (LMDOS) at the center of a quantum corral. The dotted lines indicate the maxima in the LDOS. Vertical solid lines are the energy eigenvalues,  $E_{0i}$ , predicted by the circular quantum well model (see Section 3.4).

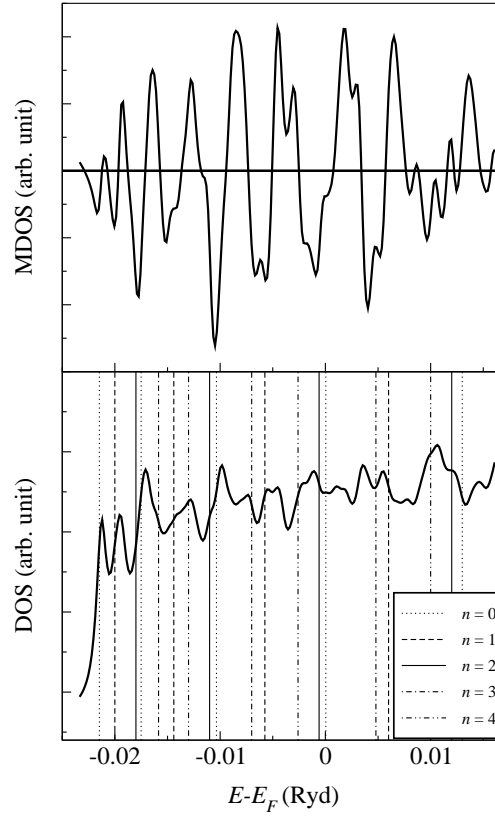


**Figure 4.** Calculated density of states (DOS) and magnetic density of states (MDOS) summed for a diameter of the corral. Vertical lines indicate the energy eigenvalues corresponding to different values of the quantumnumber  $n$  predicted by the circular quantum well model (see Section 3.4).

### 3.3. DOS of confined surface states

In order to study the properties of surface states confined by the quantum corral first we investigated the local density of states (LDOS),

$$n_i(E) = n_{i,\uparrow}(E) + n_{i,\downarrow}(E) = -\frac{1}{\pi} \sum_{\sigma=\uparrow,\downarrow} \text{ImTr} G_{\sigma\sigma}^{ii}(E) \quad , \quad (5)$$

and the local magnetic density of states (LMDOS),

$$m_i(E) = n_{i,\uparrow}(E) - n_{i,\downarrow}(E) \quad , \quad (6)$$

of an *empty sphere* at various lattice points (sites) labeled by  $i$  within the corral, where  $G_{\sigma\sigma}^{ii}(E)$  is the site- and spin-diagonal part of the resolvent in  $(\ell, m, \sigma)$  representation. Although in our relativistic theory the spin is not a good quantumnumber, and hence  $G_{\sigma\sigma'}^{ii}(E)$  is not diagonal, we can interpret the diagonal elements in a similar manner as in a non-relativistic theory, because within an empty sphere the spin-orbit coupling is bound to be small. In Figure 3 we show the LDOS and LMDOS at the center of the corral.

The striking peaky structure of the DOS in Figure 3 is in sharp contrast to the constant 2D density of states expected from the dispersion relation in Equation (4).

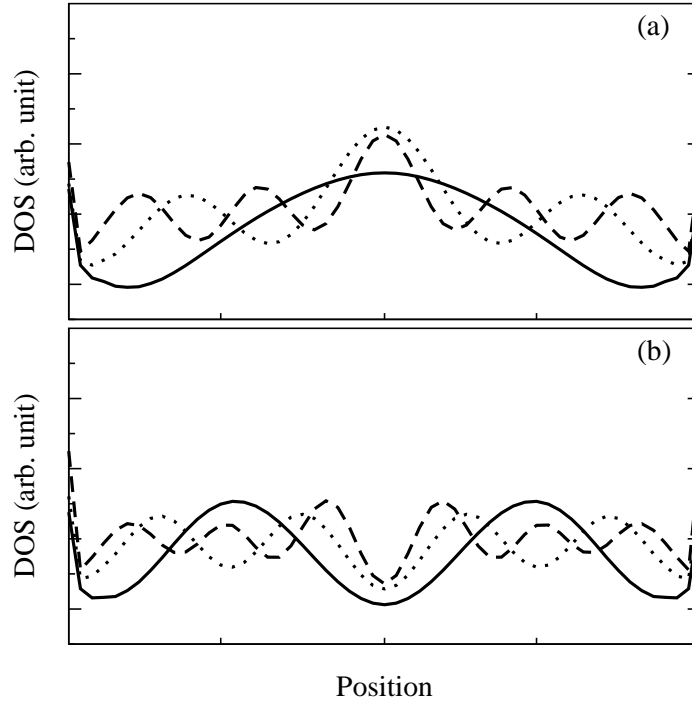


**Figure 5.** Spatial distribution of the DOS along a diameter of the quantum corral at energies corresponding to selected peaks in Figure 4. The line shapes in part (a) and (b) can be identified as  $n = 0$  and as  $n \neq 0$  quantumstates of a circular quantum well model (see Section 3.4), respectively.

However, the peaks are rather similar to those found by Crampin *et al.* [20] who interpreted them as 'bound states' within the corral. We confirm this interpretation using a simple circular well model in Section 3.5. Nevertheless, it is somewhat surprising that the coherent scattering from a circular arrangement of Fe impurities is almost equivalent to that of an infinite confining potential wall. Evidently, such confined states are analogous to the quantum well states in semiconductor physics [17]. In contrast to Crampin *et al.* [20], we have also calculated the spin-resolved densities of states (LMDOS) which are also presented in Figure 3. Clearly, the LMDOS is more structured than the LDOS suggesting that the quantum well states are exchange split. To lend further credence to such an interpretation we calculated the sum of the LDOS and LMDOS,

$$n(E) = \sum_i n_i(E) \quad , \quad m(E) = \sum_i m_i(E) \quad , \quad (7)$$

along a diameter of the corral. Note that near to the Fe atoms the LDOS increases rapidly due to the direct charge transfer, therefore, in the above sums the contributions from the empty spheres adjacent to the Fe atoms are neglected. These summed densities of states are then plotted in Figure 4. Although the peaks seen in Figure 3 are still present, Figure 4 suggests a more complex spectrum. In order to shed light on the nature of the extra states, the spatial resolution of the DOS at selected energies corresponding to the most prominent peaks are shown in Figure 5 and, for the fifth peak in Figure 3 ( $E - E_F \simeq 0.01$  Ryd), the LDOS for the whole area within the corral



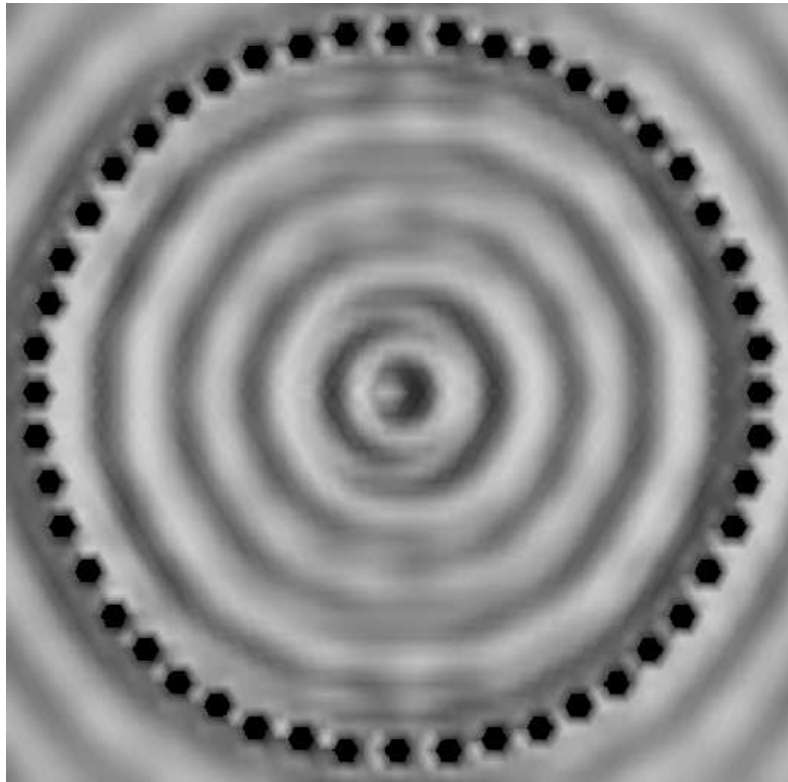


**Figure 6.** Spatial distribution of the DOS at the energy corresponding to the fifth peak of the LDOS at the central position ( $E - E_F \simeq 0.01$  Ryd). The LDOS of the Fe atoms is removed from the figure.

is depicted in Figure 6. Note that the oscillations continue outside the corral. This implies that the states, we have been studying, are really resonances rather than bound states. Reassuringly, the obtained pattern for the confined surface electrons agrees well with the experimental one [4, 5]. Beyond agreeing with experiments, the oscillations with distance from the center in Figure 5 strongly support the interpretation that the selected peak positions are those of 'bound' states confined by the corral.

Evidently, even for the present very simple geometry the full results are too complicated to allow an unambiguous identification of each structure with specific physical processes. To maximize the information gained from our first-principles calculations we shall now introduce a simple model whose parameters can be chosen such that it reproduces most of the above results quantitatively.

#### 3.4. The non-relativistic Circular Quantum Well model

The circular quantum well model is defined by a potential of the form,

$$V(\mathbf{r}) = \begin{cases} 0 & \text{if } r < R \\ +\infty & \text{if } r \geq R \end{cases} . \quad (8)$$

It should be recalled that the radial solutions of the corresponding Schrödinger equation are Bessel function of the first kind  $J_n(pr)$ , where

$$p = \sqrt{\frac{2m^*}{\hbar^2} E} \quad . \quad (9)$$

The energy eigenvalues arise from the boundary condition that the radial solutions vanish at the boundary:

$$E_{ni} = \frac{x_{ni}^2}{R^2} \frac{\hbar^2}{2m^*} \quad , \quad (10)$$

where  $x_{ni}$  refer to the  $i$ th zero of the Bessel function  $J_n$ . In order to investigate the magnetic properties of this model, one can generalize it by adding a spin-dependent part,  $V_{\uparrow(\downarrow)}(r) = V(r) + U_{i,\uparrow(\downarrow)}$ , where the constant  $U_{i,\uparrow} = -U_{i,\downarrow}$  can also depend on the quantumnumber  $n$ . The magnetic exchange term modifies the energy values as follows,

$$E_{ni}^{\uparrow(\downarrow)} = \frac{x_{ni}^2}{R^2} \frac{\hbar^2}{2m^*} + U_{i,\uparrow(\downarrow)} \quad . \quad (11)$$

In order to facilitate a comparison with the ab-initio results, the value of  $R = 27 a$  is used. This means that the radial solution has to vanish at the lattice position neighbouring the corral atoms. The corresponding energy values with and without magnetic exchange term for  $n = 0$  can be seen in Figure 7.

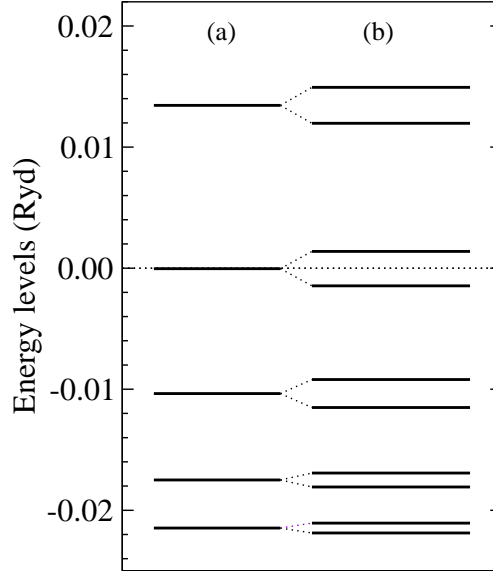


**Figure 7.** Energy levels of the  $n = 0$  states within the circular quantum well model at the radius used for the self-consistent calculation. (a): non-spinpolarized model, (b): spin-splitting term added. The energy dependent splitting between the spin-up and spin-down states is estimated from the LMDOS shown in Figure 3.

### 3.5. Interpretation of the results of first-principles calculations

In what follows we comment on the results of our first-principles calculations in the light of the above circular quantum well model. Firstly, we note that in Figure 3 the vertical solid lines correspond to the bound state energies  $E_{0i}$  for  $m^*/m_e = 0.366$  and  $U_{i,\uparrow(\downarrow)} = 0$ . The agreement between the peak positions and the  $E_{0i}$ 's is especially striking in the low-energy regime. This can be viewed as an indication that at lower energies the scatterers act more like a hard wall than at higher energies. Given that the model is solved by using the Schrödinger equation, it also suggests that relativistic effects inside the corral are not too important. In the first-principles calculations the peaks have finite widths due to the combined effects of the discreteness of the confining boundary and the energy dependent scattering into bulk states. Remarkably, the width of the peaks agrees quantitatively with the experimental values [29]. This result, however, may be fortuitous. Note, for instance, that for reasons not entirely clear, in the experiments the third peak is the highest one, but in our result the highest peak is the second one.

The spatial distribution of the DOS along a diameter of the corral is plotted in the upper panel of Figure 5 at energies referring to the first three peaks in Figure 3. As can be expected the LDOS has a maximum at the center similarly to the  $J_{n=0}$  Bessel function. The circular well model suggests that there are states with non-zero orbital moment,  $n \neq 0$ , for which there is a minimum at the center of the corral. In order to find these states, in Figure 4 we investigated the spatial sum of the LDOS along a diameter. Evidently, the  $n \neq 0$  states would contribute to this sum. Indeed, as noticed already, in Figure 4 there are new peaks as compared with Figure 3 to which states with zero amplitude at the center do not contribute. In Figure 4, the values  $E_{ni}$  as predicted from the circular quantum well model with zero exchange-split term,  $U_{i,\uparrow(\downarrow)} = 0$ , are also indicated by vertical lines up to  $n = 4$ . Note, for example, that the second peak clearly corresponds to the  $n = 1, i = 1$  quantum state. To pursue this matter further, in the lower panel of Figure 5, we plotted the spatial density of the states corresponding to those peaks which appear only in the summed DOS. Reassuringly, these spatial densities have minimum at the center. For higher energies this correspondence is not so clear, nevertheless, this comparison serves as an explanation why the shape of the peaks differs from that of an ideal Lorentzian. The small features between the prominent peaks which can be seen in Figure 3, and in the experimental results [4] also show some systematic trends which we assume can be explained in terms of a the circular quantum well model based on a two-dimensional Dirac equation.

Turning to the LMDOS at the central position, we note that in the upper panel in Figure 3 the prominent DOS peaks are split into a pair of 'up' and 'down' peaks. This oscillatory behaviour of the LMDOS is a consequence of the spin-polarization of the corral Fe atoms, namely of the perturbation of the surface-state electrons by the Fe atoms forming the corral. This exchange splitting can be reproduced in the circular well model by choosing  $U_{i,\uparrow(\downarrow)}$  appropriately. It turns out that for a good fit  $U_{i,\uparrow(\downarrow)}$  should be non-uniform in energy. The corresponding energy values with the exchange splitting terms estimated from Figure 3 are shown in Figure 7b. Thus, the prediction of the model is that if the Fermi energy falls between an exchange-split doublet then the whole corral has a net magnetic moment of one Bohr magneton in addition to the magnetization due to the Fe atoms forming the wall. Furthermore, such a moment will not be uniformly distributed within the corral but varies from empty-cell to empty-

cell as required by the wavefunction of the confined surface state, namely, it oscillates like the charge density in Figure 5. Of course, even for a relatively small corral of  $R = 27 a$ , as indicated by the highly structured summed LMDOS in the upper panel of Figure 4, there are many states near the Fermi energy and hence the local magnetic moment can vary rapidly with Fermi energy and spatial location. Some of the complexities in this figure can be attributed to the appearance of the  $n \neq 0$  states. Although the exchange splitting around the DOS peaks can be clearly observed, a full analysis of the results of our relativistic spin-polarized ab-initio calculations will have to be based on a relativistic treatment of the circular well model.

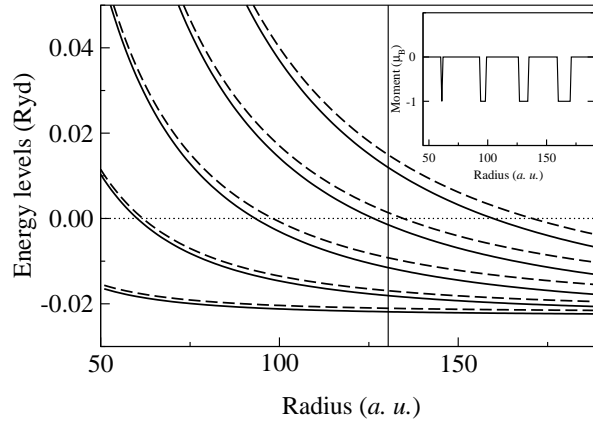


**Figure 8.** The  $n = 0$  energy levels with spin-splitting (dashed line: spin-up states, solid lines: spin-down states). Inset: Value of the magnetization with respect to the radius within the circular quantum well model due to the  $n = 0$  states. The energy dependent splitting between the spin-up and spin-down states is estimated from the MDOS calculations. The vertical line indicates the radius used for the first-principles calculation.

### 3.6. Tuning of the magnetic properties

From the point of view of engineering corrals with specific properties it is important to investigate the magnetic properties of the confined surface states within the corral as a function of the corral radius  $R$ . As a preliminary effort in this direction we shall now make some estimates based on the model whose credibility we have established in the previous sections. Firstly, we have calculated the dependence of the exchange split energy levels, shown in Figure 7 for the specific case of  $R = 130.41 a.u.$ , as a function of  $R$ . The results are displayed in Figure 8. Assuming that the exchange energies are independent from the geometry we used the values estimated from Figure 3. It can be seen that as the radius is decreased the energy levels are pushed upwards, possibly changing the number of the occupied states. As a consequence of this effect one can find ranges of radii where the spin-down state is occupied but the corresponding spin-up state is empty and, therefore, the surface states hold a finite magnetic moment. The predicted total magnetic moment of the surface states is depicted in the inset of Figure 8. It should be stressed that the model neglects a multitude of effects such as the partial confinement of the electrons and the width of the levels. In realistic first-principles calculations the magnetic moment is expected to show a smoother change

with the radius. When states with  $n > 0$  are also taken into account the results are expected to be even more complicated but, qualitatively, the basic effect should remain the same. For instance, at the center of the corral one can expect from Figure 4 that it is enough to take into account the  $n = 0$  states. Therefore, we can predict that at least at the center there is a finite magnetic moment at well defined geometries. In short, by varying the geometry a rich variety of magnetic states can be produced.

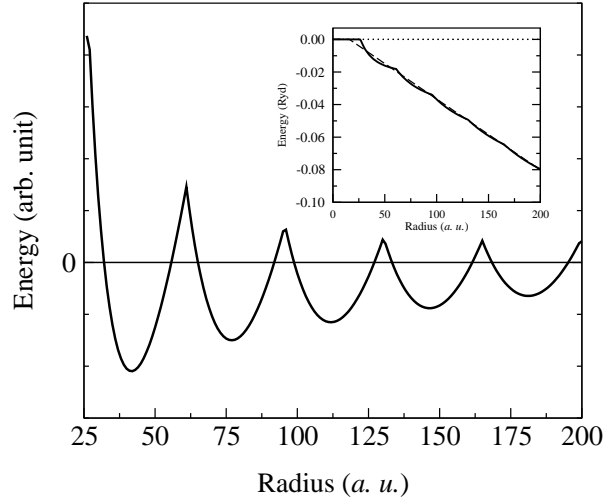


**Figure 9.** Oscillation in the total energy with respect to the radius of the corral within the circular quantum well model due to the  $n = 0$  states. In the inset, the total energy and its best linear fit ( $R > 25 a.u.$ ) are plotted by solid and dashed line, respectively. In the main figure, the difference between the total energy and its linear fit are depicted for a better representation of the oscillations.

As might be expected by now the total energy also shows an interesting behaviour by varying the corral radius. As a simple, and perhaps artificial, example we have studied the case when symmetry constrains the system such that only the  $n = 0$  states are occupied. The total energy for this case is shown in Figure 9. The oscillations resemble and have similar origin as those responsible for the de Haas–van Alphen effect. Note, however, that in the present example the oscillations are not equally spaced but follow from the distribution of the Bessel zeros. Interestingly, similar oscillations can be expected if, instead the radius  $R$ , the Fermi energy  $E_F$  changes. In an experiment one may contrive such variations in  $E_F$  by ‘gating’ the corral with an STM tip.

#### 4. Summary

In this work we presented calculations of the electronic and magnetic properties of the surface states confined in a circular quantum corral. The ab-initio results are interpreted in terms of a simple quantum mechanical, circular potential well model with infinitely high walls. We found that at low energies the energy levels of the model gave a good quantitative account of the peaks of the DOS obtained in ab-initio calculations. In particular, unlike previous calculations for the quantum corrals, we were able to study and interpret the magnetic as well as the charge oscillations within the corral. On the basis of these calculations we conclude that a rich variety of magnetic

structures can be expected by varying the shape, size and gating of these fascinating nanostructures.

## Acknowledgments

Financial support was provided by the Center for Computational Materials Science (Contract No. GZ 45.531), the Austrian Science Foundation (Contract No. W004), the Research and Technological Cooperation Project between Austria and Hungary (Contract No. A-3/03) and the Hungarian National Scientific Research Foundation (OTKA T046267 and OTKA T037856). The work of BU was supported by DOE-OS, BES-DMSE under contract number DE-AC05-00OR22725 with UT-Battelle LLC.

## References

- [1] Kevan S D 1983 *Phys. Rev. Lett.* **50** 526
- [2] Hörmandinger G and Pendry J. B 1994 *Phys. Rev. B* **50** 18607
- [3] Baumberger F, Greber T and Osterwalder J 2001 *Phys. Rev. B* **64**, 195411
- [4] Crommie M F, Lutz C P, Eigler D M and Heller E J 1995 *Physica D* **83** 98
- [5] Crommie M F, Lutz C P, Eigler D M and Heller E J 1996 *Surf. Sci.* **361/362** 864
- [6] Manoharan H C, Lutz C P and Eigler D M 2000 *Nature* **403** 512
- [7] Bode M 2003 *Rep. Prog. Phys.* **65** 523
- [8] Pietzsch O, Kubetzka A, Bode M and Wiesendanger R 2004 *Phys. Rev. Lett.* **92** 057202
- [9] Petersen L, Sprunger P T, Hofmann Ph, Laegsgaard E, Briner B G, Doering M, Rust H-P, Bradshaw A M, Besenbacher F and Plummer E W 1998 *Phys. Rev. B* **57** R6858
- [10] Diekhöner L, Schneider M A, Baranov A N, Stepanyuk V S, Bruno P and Kern K 2003 *Phys. Rev. Lett.* **90** 236801
- [11] Repp J, Moresco F, Meyer G and Rieder K-H 2000 *Phys. Rev. Lett.* **85** 2981
- [12] Knorr N, Brune H, Epple M, Hirstein A, Schneider M A and Kern K 2002 *Phys. Rev. B* **65** 115420
- [13] Stepanyuk V S, Baranov A N, Tsivlin D V, Hergert W, Bruno P, Knorr N, Schneider M A and Kern K 2003 *Phys. Rev. B* **68** 205410
- [14] Porrás D, Fernández-Rossier J and Tejedor C 2001 *Phys. Rev. B* **63** 155406
- [15] Fiete G A, Hersch J S, Heller E J, Manoharan H C, Lutz C P and Eigler D M 2001 *Phys. Rev. Lett.* **86** 2392
- [16] Agam O and Schiller A 2001 *Phys. Rev. Lett.* **86** 484
- [17] Wang S 1989 *Fundamentals of Semiconductors Theory and Device Physics* (Prentice Hall, Inc., Englewood Cliffs)
- [18] Fiete G A and Heller E J 2003 *Phys. Rev. Lett.* **75** 933
- [19] Doron E and Smilansky U 1992 *Nonlinearity* **5** 1055
- [20] Crampin S and Bryant O R 1996 *Phys. Rev. B* **54** R17367
- [21] Crampin S, Boon M H and Inglesfield J E 1994 *Phys. Rev. Lett.* **73** 1015; Harbury H K and Porod W 1996 *Phys. Rev. B* **53** 15455; Crampin S 2000 *J. Electron. Spectrosc. Relat. Phenom.* **109** 51; Kliewer J, Berndt R and Crampin S 2000 *Phys. Rev. Lett.* **85** 4936; Kliewer J, Berndt R and Crampin S 2001 *New J. Phys.* **3**, 22
- [22] Crommie M F, Lutz C P and Eigler D M 1993 *Nature* **363** 524
- [23] For more details, especially, how to calculate  $t_{QQ'}^n(E)$  within a fully relativistic spin-polarized scheme, see, e.g., Weinberger P 1990 *Electron Scattering Theory for Ordered and Disordered Matter* (Clarendon, Oxford)
- [24] Lazarovits B, Szunyogh L and Weinberger P 2002 *Phys. Rev. B* **65** 104441
- [25] Szunyogh L, Újfalussy B and Weinberger P 1995 *Phys. Rev. B* **51** 9552
- [26] Lazarovits B, Szunyogh L, Weinberger P and Újfalussy B 2003 *Phys. Rev. B* **68** 024433
- [27] Vosko S H, Wilk L and Nusair M 1980 *Can. J. Phys.* **58** 1200
- [28] Bruno P 1993 *Physical Origins and Theoretical Models of Magnetic Anisotropy*, in 24. Ferienkurse des Forschungszentrum Jülich (eds. Dederichs P H, Grünberg P and Zinn W, Jülich)
- [29] Crommie M F, Lutz C P and Eigler D M 1993 *Science* **262** 5131